JACS
JOURNAL OF THE AMERICAN CHEMICAL SOCIETY
Communication
pubs.acs.org/JACS

Electrochemical Tip-Enhanced Raman Spectroscopy

Zhi-Cong Zeng,[†] Sheng-Chao Huang,[†] De-Yin Wu,[†] Ling-Yan Meng,[‡] Mao-Hua Li,[†] Teng-Xiang Huang,[†] Jin-Hui Zhong,[†] Xiang Wang,[†] Zhi-Lin Yang,[‡] and Bin Ren*[,†]

[†]State Key Laboratory of Physical Chemistry of Solid Surface, The MOE Key Laboratory of Spectrochemical Analysis & Instrumentation, Collaborative Innovation Center of Chemistry for Energy Materials (*i*ChEM), College of Chemistry and Chemical Engineering, and [‡]Department of Physics, Xiamen University, Xiamen 361005, China

Supporting Information

ABSTRACT: Interfacial properties are highly important to the performance of some energy-related systems. The in-depth understanding of the interface requires highly sensitive in situ techniques that can provide fingerprint molecular information at nanometer resolution. We developed an electrochemical tip-enhanced Raman spectroscopy (EC-TERS) by introduction of the light horizontally to the EC-STM cell to minimize the optical distortion and to keep the TERS measurement under a well-controlled condition. We obtained potential-dependent EC-TERS from the adsorbed aromatic molecule on a Au(111) surface and observed a substantial change in the molecule configuration with potential as a result of the protonation and deprotonation of the molecule. Such a change was not observable in EC-SERS (surface-enhanced), indicating EC-TERS can more faithfully reflect the fine interfacial structure than EC-SERS. This work will open a new era for using EC-TERS as an important nanospectroscopy tool for the molecular level and nanoscale analysis of some important electrochemical systems including solar cells, lithium ion batteries, fuel cells, and corrosion.

Revealing the nature of interfacial properties, including the chemical identity of surface species, adsorbate−substrate and adsorbate−adsorbate interactions, spatial arrangement of adsorbates on surfaces, and electronic properties of the surface, is fundamentally significant in the development of molecular electronics, perovskite solar cells, fuel cells, lithium ion batteries, corrosion, chemical sensors, etc. Although the number of species in the interface is negligible in comparison with that in the bulk phase, the performance of most devices is determined by the interfacial properties.

Discovery of surface-enhanced Raman spectroscopy (SERS) in the 1970s[1−3] offered a highly sensitive tool to the surface science community, with high interfacial sensitivity, down to single molecules.[4,5] The problem associated with SERS, the need for nanostructure surfaces to provide the enhancement, has been partially overcome by the shell-isolated nanoparticle-enhanced Raman spectroscopy (SHINERS).[6] With SHINERS, surface Raman studies have been extended to single-crystal surfaces that do not support a surface enhancement effect. If the surface Raman study can be performed without any contact and at a spatial resolution breaking the diffraction limits, it will be highly important to the field. In this regard, tip-enhanced Raman spectroscopy (TERS) is particularly interesting.[7−11] It follows the same enhancement mechanisms as SERS by replacing the multiple SERS hot spots with a single well-defined hot spot formed by the Au or Ag tips controlled by scanning probe microscopy (SPM).[12] In such a configuration, the electromagnetic field is highly confined to the vicinity of the tip apex, offering a single-molecule sensitivity[13−16] and a submolecular spatial resolution.[17] The development of ultrahigh vacuum and ultra-low-temperature TERS (UHV-TERS) has not only significantly improved the stability and imaging quality of TERS but also solved the contamination problem interfering with the surface process on single-crystal surfaces.

However, TERS working under the ambient or UHV condition can only partially meet the requirement for characterization of the interfacial structure of real systems. In an electrochemical system, the interfacial process and structure can be precisely controlled by changing the electrode potential (thus the Fermi level of the electrode). Once the potential control or electrolyte is disconnected, the interfacial processes will change and the interfacial structure may relax to the state at the open-circuit potential and will be different from the potential of interest. Therefore, there is an increasing interest in developing electrochemical TERS (EC-TERS) for characterization of important interfaces,[18−20] especially a scanning tunneling microscopy (STM)-based method, because STM can provide high spatial resolution. As far as we know, there was only one TERS report in liquid but not under EC condition.[21]

EC-TERS involves the combination of SPM, plasmon-enhanced Raman spectroscopy, and electrochemistry in a setup. Therefore, it is very challenging to develop STM-based EC-TERS to couple the optical system into the limited space of a STM. Especially when an opaque bulk electrode (e.g., single crystal) is used, one has to work in a side-illumination mode, in which it is impractical to use a high numerical aperture (NA) objective (usually oil- or water-immersion) with a short working distance. In this mode, the light has to pass through the air and the electrolyte of different refractive index in a tilted way, and the optical path will be severely distorted (see Figure S1 for details). Therefore, it is almost impossible to form a good focus, especially when the electrolyte layer becomes thicker.

To overcome the problem, we report here an STM-based EC-TERS. The setup is illustrated in Figure 1a. The electronic part is the same as the EC-STM, where the potentials of the tip (WE1)

Received: August 3, 2015
Published: September 9, 2015

DOI: 10.1021/jacs.5b08143
J. Am. Chem. Soc. 2015, 137, 11928−11931

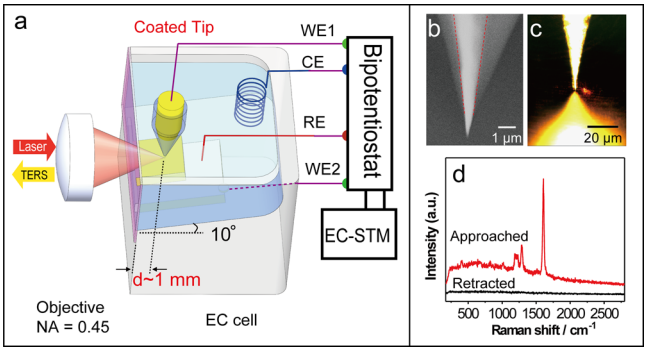

Figure 1. (a) Schematic illustration of the EC-TERS setup. (b) SEM image of an insulated gold tip. (c) Microscopic image of the tip, single-crystal substrate, and laser spot in an EC-TERS system. (d) TERS of 4-PBT adsorbed on the Au(111) surface obtained while the tip was approached (top) and retracted (bottom). The acquisition time was 1 s. The bias voltage was 500 mV, and the tunneling current was 500 pA.

and the substrate (WE2) are controlled by a bipotentiostat relative to a Pt wire. The laser is introduced horizontally via a long working distance microscope objective (NA = 0.45) to the electrochemical cell and illuminated in the gap of the tip and Au(111) surface. The produced TERS signal is collected by the same objective and sent to a home-built Raman system for detection (see Figure S2 for detailed optical path). To ensure a high throughput, we modified the EC-STM cell by tilting the single crystal to about 10°, so that the laser can be properly focused onto the tip and the Raman signal can be collected with high efficiency. In this configuration, the tip can still approach vertically downward. It appears that 10° is a sweet balance to keep the high imaging quality of STM and high collection efficiency of the Raman system, without much modification of the STM system. Benefitted from this design, the optical path will not change compared with that of tilted illumination even if there is evaporation of the electrolyte during the EC-TERS measurement, allowing a long time measurement.

It is known in the STM-based TERS that the tip plays dual roles: to produce the enhanced electromagnetic field and to allow the pass of the tunneling current. However, in EC-TERS, an extra problem has to be considered because the tip may produce Faradaic current. Therefore, different from the TERS measurement in air or vacuum, the tip has to be insulated in EC-TERS so that the Faradaic current produced on the tip will not interfere with the tunneling current used to control the STM.[22] Furthermore, different from EC-STM, the tip insulation materials should not produce the Raman or fluorescence background. For this purpose, we chose polyethylene glue (Rapid Pro+, Sweden) as the insulating materials. The SEM image of the tip end after coating is shown in Figure 1b. The bright part is the Au tip, and the gray part is the insulating materials. It is obvious that the glue forms a very nice cone shape and tapers to the tip end. The exposed length of the tip is about 1 μm, which is almost of the same size of the laser spot. The leakage current in EC-STM is less than 50 pA, which will not interfere with the tunneling current. When the tip approached the single-crystal surface, a very clear tip and the broadened tip image (due to the tilted substrate) were observed. When the laser was moved outside the gap region, a clear laser spot was observed (see Figure 1c). It indicates a nice tip coating as well as a nice imaging quality of the optical system. In this work, we chose 4-PBT ((4′-(pyridin-4-yl)biphenyl-4-yl)methanethiol),[23] an important molecule in molecular electronics, as a model molecule for EC-TERS study. When the insulated tip approached a Au(111) single-crystal surface adsorbed with 4-PBT molecules in an electrochemical system, a strong TERS signal was observed, whereas, when the tip was retracted, no signal could be obtained (see Figure 1d). We can conclude that the tip will not produce an interfering signal to TERS and can be successfully used for EC-TERS measurement.

We then demonstrated the advantage of EC-TERS by measuring the time series TERS in the electrochemical system (Figure 2a) and in air (Figure 2b). The intensity and frequency of

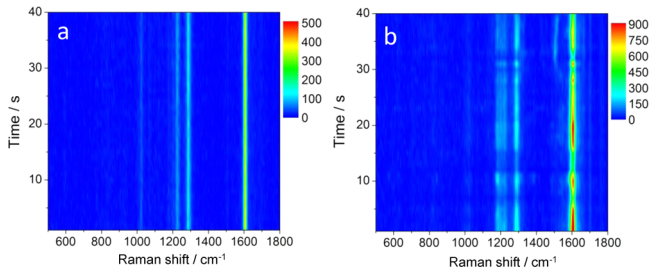

Figure 2. Time series TERS signal of 4-PBT adsorbed on the Au(111) surface obtained (a) in 0.1 M $NaClO_4$ (pH 3) at an electrode potential of −500 mV in a 10° configuration and (b) in air in a 30° configuration. The acquisition time was 1 s. The bias voltage was 500 mV, and the tunneling current was 200 pA.

the TERS signal obtained under the EC condition almost remain unchanged throughout the experiment (Figure 2a), whereas the TERS signal obtained in air fluctuates quite obviously and some new peaks appears. The signal even weakens toward the extension of the experiment. It is clear that the EC-TERS signal is more stable compared with that obtained in air, which may be due to the following reasons: (1) For TERS in air, some impurities may attach to the gap of the tip and substrate. (2) Oxygen in air may be activated to induce the photochemical reaction under laser illumination at the plasmonic gap.[24,25] (3) Excitation of localized surface plasmon resonance will lead to the elevation of the temperature in the gap, resulting in desorption of the molecule. These problems can be effectively overcome when the measurement is performed in the electrochemical system. The electrolyte is a buffer to prevent exposure of the plasmonically active tip−substrate gap to air and impurities, and high heat capacity of water can effectively prevent the abrupt rise of the local temperature. Furthermore, EC-TERS can tune the surface properties to enhance the interaction of the molecule with the substrate, which is advantageous compared with the normal TERS.

With the advantage of the EC-TERS in mind, we then systematically carried out the EC-TERS study of the above system. The STM image of a Au(111) surface adsorbed with 4-PBT molecules is shown in Figure 3a. The image shows clear terraces of the single-crystal surface. The molecule forms a compact self-assembled monolayer on the Au surface via the gold−sulfur bond, with only some defects on the surface. The STM image indicates that, after modification, the EC-STM can still give a reasonably good imaging quality. The cyclic voltammogram (CV) of the substrate is shown as the red curve in Figure 3b. The CV shows a wide potential window (−0.7 to +0.3 V), which can be conveniently used to study the change of the interfacial structure in the absence of electrochemical reactions. In contrast, the bare Au(111) surface shows a complicated electrochemical response in the whole potential

DOI: 10.1021/jacs.5b08143
J. Am. Chem. Soc. 2015, 137, 11928−11931

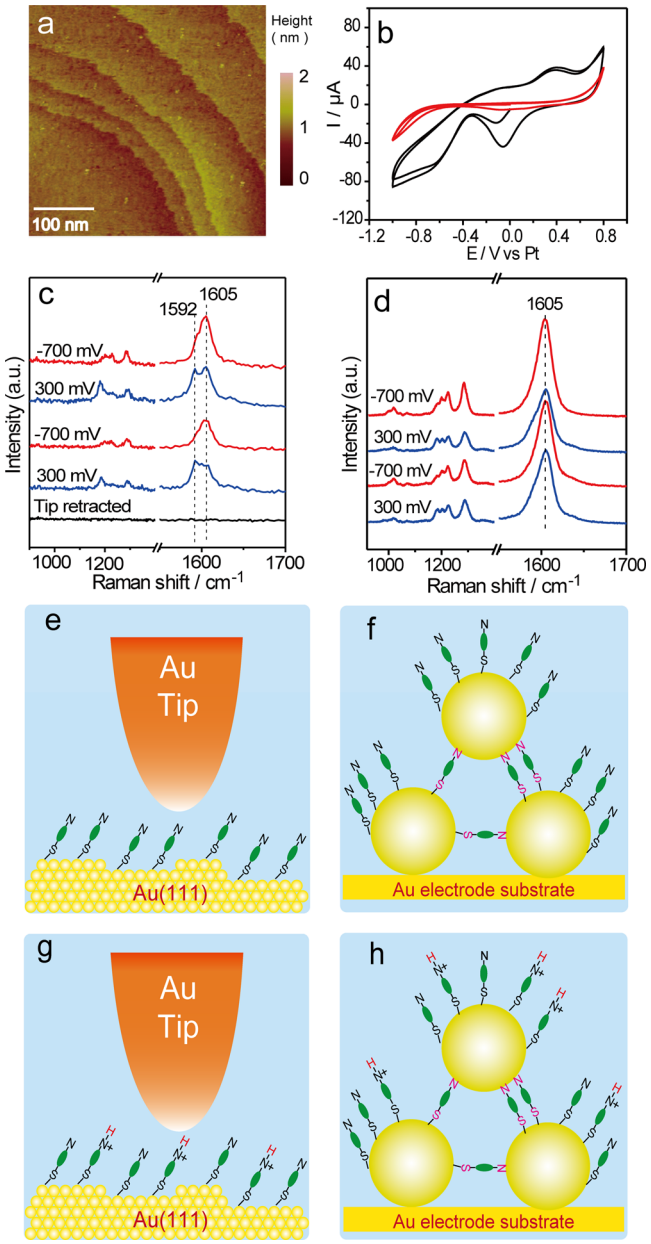

Figure 3. (a) STM image of a 4-PBT-adsorbed Au(111) surface. The bias voltage was 500 mV, and the tunneling current was 500 pA. (b) CVs of a bare (black) and 4-PBT-adsorbed (red) Au(111) electrode in 0.1 M $NaClO_4$ (pH 10). The scan rate is 0.1 V/s. (c) Potential-dependent EC-TERS of 4-PBT adsorbed on the Au(111) surface. Tip potential was −200 mV, and the tunneling current was 500 pA. (d) Potential-dependent SERS of a 4-PBT-modified Au NP surface. The acquisition time was 3 s for TERS and 1 s for SERS. The solution was 0.1 M $NaClO_4$ (pH 10). (e,g) Models for the TERS system at positive and negative potentials, respectively. (f,h) Models for the SERS system at positive and negative potentials, respectively.

range, where the surface oxidation and hydrogen evolution occur on the surface. By comparing the two CVs, we conclude that the 4-PBT molecule passivates the surface.

Figure 3c shows potential-dependent EC-TERS. The TERS obtained while the tip was retracted is also shown for comparison. At 0.3 V, we can observe doublet peaks at 1592 and 1605 cm^{-1}, whereas the low-frequency peak weakens and only appears as a shoulder peak at −0.7 V (the potential of zero charge of the 4-PBT-modified Au(111) surface is about −0.4 V; see Figure S4). To understand this behavior, we also performed the SERS study of the same system, but with Au nanoparticles as the SERS substrate. Surprisingly, the EC-SERS (Figure 3d) show features much different than that of the EC-TERS. We can only observe a single peak at 1605 cm^{-1}. According to our density functional theory (DFT) calculation, the 1592 cm^{-1} is contributed by the pyridine ring and 1605 cm^{-1} is contributed by the benzene ring (see Figure S9 and Table S1). Therefore, we propose that when the N end of the 4-PBT molecule is protonated (see Figure 3e,g), the peak will shift to a high frequency to overlap with the 1605 cm^{-1} and appears as a single peak. In the case of SERS, some 4-PBT molecules may be trapped between the nanoparticles to form double-end-bonded 4-PBT molecules (Figure 3f,h). Such a double-end-bonded species may have a frequency close to that of the protonated 4-PBT molecules (can also be considered double-end-bonded). Furthermore, the trapped molecules are in the gap of nanoparticles and experience the strongest enhancement, which will contribute to the majority of the Raman signal. Therefore, there are even some single-end-bonded 4-PBT molecules on the surface; the protonated form will not have an obvious contribution to the total SERS signal.

To prove this assumption, we performed an EC-TERS study (see Figure 4a) in solution at pH 3.0 (the pK_a of 4-PBT was 5.0 ± 0.5),[26] so the majority of the 4-PBT molecules are in the protonated form. Indeed, we only observed a single peak at 1607 cm^{-1} regardless of positive or negative potentials. The spectral feature is similar to the TERS at negative potentials at pH 10 and similar to the SERS. This result convincingly demonstrates that protonation is responsible for the observation of different spectral features for the molecule at positive and negative potentials. Our DFT calculation (see Figure 4b) of the molecules in different states further supports the above assumption. The single-end-bonded species gives a major peak in the high-frequency side and a shoulder peak in the low-frequency side, whereas both protonated and double-end-bonded species produce only a single peak. From the above result, we find that EC-TERS can more sensitively reflect the interfacial structure of an electrochemical system, due to the simple and well-defined configuration and much fewer detected molecules (<600). It

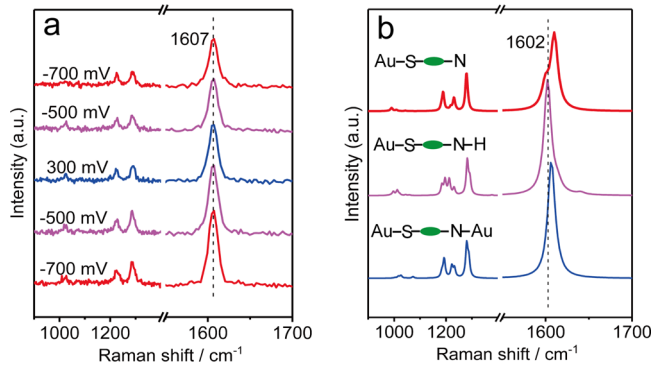

Figure 4. (a) Potential-dependent EC-TERS of 4-PBT adsorbed on the Au(111) surface in 0.1 M $NaClO_4$ (pH 3). Tip potential was −200 mV, and the tunneling current was 200 pA. The acquisition time was 1 s. (b) DFT calculation of the Raman spectra of 4-PBT molecules in different states: single-end-bonded 4-PBT on Au (top), protonated 4-PBT on Au (middle), and double-end-bonded 4-PBT (Au-4-PBT-Au, bottom). The calculation considered the solvation effect using the polarizable medium model. A scaling factor of 0.981 was used.

DOI: 10.1021/jacs.5b08143
J. Am. Chem. Soc. 2015, 137, 11928−11931

reveals some interfacial structural change that is submerged by the complicated configuration (multiple hot spot sites) in EC-SERS, offering itself as a highly sensitive method for reliable characterization of an electrochemical system. This technique offers a unique chance to address more interesting and challenging issues in energy-related electrochemical systems.

In summary, we have developed an electrochemical tip-enhanced Raman spectroscopy, a promising nanospectroscopy, by integrating a commercial STM system with a home-built confocal Raman microscope using horizontal illumination mode. We obtained potential-dependent electrochemical TERS signals from monolayer species on Au(111) single-crystal surfaces that can more faithfully reflect a very subtle change in the molecular configuration with the change of the potential compared with EC-SERS. The presence of the water layer not only prevents the contamination from air but also improves the spectral stability compared with that of the ambient TERS. EC-TERS further provides us the flexibility to control the potential to tune the plasmon resonance frequency as well as the interaction of the molecule with the substrate. With further improvement of the detection sensitivity, we may eventually be able to perform nanoscale spectral imaging of the electrochemical interfaces, which is a long-term dream for surface sciences. In particular, with the extremely high spatial resolution down to several nanometers and high sensitivity down to the single-molecule level, EC-TERS will become an unprecedented tool for the molecular level and nanoscale analysis of some important electrochemical systems related to solar cells, lithium ion batteries, and fuel cell systems.

■ ASSOCIATED CONTENT

Supporting Information

The Supporting Information is available free of charge on the ACS Publications website at DOI: 10.1021/jacs.5b08143.

Optical distortion, experimental condition, preparation of the sample and tip, tip coating method, experimental procedures for performing the EC-TERS, TERS with opposite polarity of bias, EC-SERS obtained in the solution of pH 3, FDTD solution calculation, and DFT calculation (PDF)

■ AUTHOR INFORMATION

Corresponding Author

*bren@xmu.edu.cn

Notes

The authors declare no competing financial interest.

■ ACKNOWLEDGMENTS

We acknowledge support from MOST (2011YQ03012406), NSFC (21227004, 21321062, and J1310024), and MOE (IRT13036). We gratefully acknowledge Prof. Terfort for providing 4-PBT molecules.

■ REFERENCES

(1) Fleischmann, M.; Hendra, P. J.; Mcquillan, A. J. *Chem. Phys. Lett.* **1974**, *26*, 163.
(2) Albrecht, M. G.; Creighton, J. A. *J. Am. Chem. Soc.* **1977**, *99*, 5215.
(3) Jeanmaire, D. L.; Van Duyne, R. P. *J. Electroanal. Chem. Interfacial Electrochem.* **1977**, *84*, 1.
(4) Kneipp, K.; Wang, Y.; Kneipp, H.; Perelman, L. T.; Itzkan, I.; Dasari, R.; Feld, M. S. *Phys. Rev. Lett.* **1997**, *78*, 1667.
(5) Nie, S. M.; Emory, S. R. *Science* **1997**, *275*, 1102.
(6) Li, J. F.; Huang, Y. F.; Ding, Y.; Yang, Z. L.; Li, S. B.; Zhou, X. S.; Fan, F. R.; Zhang, W.; Zhou, Z. Y.; Wu, D. Y.; Ren, B.; Wang, Z. L.; Tian, Z. Q. *Nature* **2010**, *464*, 392.
(7) Anderson, M. S. *Appl. Phys. Lett.* **2000**, *76*, 3130.
(8) Hayazawa, N.; Inouye, Y.; Sekkat, Z.; Kawata, S. *Opt. Commun.* **2000**, *183*, 333.
(9) Pettinger, B.; Picardi, G.; Schuster, R.; Ertl, G. *Electrochemistry (Tokyo, Jpn.)* **2000**, *68*, 942.
(10) Sanchez, E. J.; Novotny, L.; Xie, X. S. *Phys. Rev. Lett.* **1999**, *82*, 4014.
(11) Stockle, R. M.; Suh, Y. D.; Deckert, V.; Zenobi, R. *Chem. Phys. Lett.* **2000**, *318*, 131.
(12) Wessel, J. *J. Opt. Soc. Am. B* **1985**, *2*, 1538.
(13) Neacsu, C. C.; Dreyer, J.; Behr, N.; Raschke, M. B. *Phys. Rev. B: Condens. Matter Mater. Phys.* **2006**, *73*, 193406.
(14) Zhang, W.; Yeo, B. S.; Schmid, T.; Zenobi, R. *J. Phys. Chem. C* **2007**, *111*, 1733.
(15) Steidtner, J.; Pettinger, B. *Phys. Rev. Lett.* **2008**, *100*, 236101.
(16) Sonntag, M. D.; Klingsporn, J. M.; Garibay, L. K.; Roberts, J. M.; Dieringer, J. A.; Seideman, T.; Scheidt, K. A.; Jensen, L.; Schatz, G. C.; Van Duyne, R. P. *J. Phys. Chem. C* **2012**, *116*, 478.
(17) Zhang, R.; Zhang, Y.; Dong, Z. C.; Jiang, S.; Zhang, C.; Chen, L. G.; Zhang, L.; Liao, Y.; Aizpurua, J.; Luo, Y.; Yang, J. L.; Hou, J. G. *Nature* **2013**, *498*, 82.
(18) Tian, Z. Q.; Ren, B. Raman Spectroscopy of Electrode Surfaces. In *Encyclopedia of Electrochemistry*; Bard, A. J., Stratmann, M., Unwin, P., Eds.; Wiley-VCH: Weinheim, Germany, 2003; Vol. 3, pp 572−659.
(19) Pettinger, B. Tip-Enhanced Raman Spectroscopy: Recent Developments and Future Prospects. In *Advances in Electrochemical Science and Engineering*; Alkire, R. C., Tobias, C. W., Eds.; John Wiley & Sons: New York, 2008; Vol. 5, pp 377−411.
(20) Tian, Z. Q.; Ren, B. *Annu. Rev. Phys. Chem.* **2004**, *55*, 197.
(21) Schmid, T.; Yeo, B. S.; Leong, G.; Stadler, J.; Zenobi, R. *J. Raman Spectrosc.* **2009**, *40*, 1392.
(22) Nagahara, L. A.; Thundat, T.; Lindsay, S. M. *Rev. Sci. Instrum.* **1989**, *60*, 3128.
(23) Schüpbach, B.; Terfort, A. *Org. Biomol. Chem.* **2010**, *8*, 3552.
(24) Huang, Y. F.; Zhang, M.; Zhao, L. B.; Feng, J. M.; Wu, D. Y.; Ren, B.; Tian, Z. Q. *Angew. Chem., Int. Ed.* **2014**, *53*, 2353.
(25) Wu, D. Y.; Zhang, M.; Zhao, L. B.; Huang, Y. F.; Ren, B.; Tian, Z. Q. *Sci. China: Chem.* **2015**, *58*, 574.
(26) Muglali, M. I.; Bashir, A.; Terfort, A.; Rohwerder, M. *Phys. Chem. Chem. Phys.* **2011**, *13*, 15530.

DOI: 10.1021/jacs.5b08143
J. Am. Chem. Soc. 2015, 137, 11928−11931